On the hand-over-hand mechanism of kinesin

Qiang Shao and Yi Qin Gao*

Department of Chemistry, Texas A&M University, College Station, TX 77843

Communicated by Rudolph A. Marcus, California Institute of Technology, Pasadena, CA, April 6, 2006 (received for review December 8, 2005)

We present here a simple theoretical model for conventional kinesin. The model reproduces the hand-over-hand mechanism for kinesin walking to the plus end of a microtubule. A large hindering force induces kinesin to walk slowly to the minus end, again by a hand-over-hand mechanism. Good agreement is obtained between the calculated and experimental results on the external force dependence of the walking speed, the forward/backward step ratio, and dwell times for both forward and backward steps. The model predicts that both forward and backward motions of kinesin take place at the same chemical state of the motor heads, with the front head being occupied by an ATP (or ADP,P_i) and the rear being occupied by an ADP. The direction of motion is a result of the competition between the power stroke produced by the front head and the external load. The other predictions include the external force dependence of the chemomechanical coupling ratio (e.g., the stepping distance/ATP ratio) and the walking speed of kinesin at force ranges that have not been tested by experiments. The model predicts that the chemomechanical coupling remains tight in a large force range. However, when the external force is very large (e.g., ≈18 pN), kinesin slides in an inchworm fashion, and the translocation of kinesin becomes loosely coupled to ATP turnovers.

backward walking | chemomechanical coupling

Kinesins are linear motors that are widely distributed in almost all eukaryotic cells, and there are 45 different kinesin species in humans (1). These microtubule-based motors are involved in many functions of biological systems, including cargo transport, mitosis, and control of microtubule dynamics, and they play important roles in signal transduction pathways (1–5). Kinesins are further classified into three categories: N-terminal kinesins, C-terminal kinesins, and M kinesins, with the first being the majority in humans (2). The motions of the kinesins on microtubules are directional: N-terminal kinesins move to the plus end of the microtubule, and C-terminal kinesins move toward the minus end of the microtubule (1, 2). Kinesins have a large variety of structures, and they function as monomers, dimers, or tetramers in cells (1, 2). Among the family members of kinesins, the only conserved region is the catalytic core (5).

Conventional kinesin is a homodimer, and each of the monomers contains a heavy chain of ≈120 kDa (1). The essential structural elements of a kinesin monomer include an N-terminal motor head, which contains the nucleotide-binding site, a neck linker, a long coiled coil that is responsible for dimerization, and a globular cargo-binding tail domain formed by a light chain (1, 2, 5). The motor domain also contains the microtubule-binding site. In forming a dimer, the long coiled coils form a central stalk. The neck linker is an extension from the motor head and is assumed (1, 3, 4) to serve as a lever arm in force generation. Structural studies indicate that the conformation of the neck linkers changes in a nucleotide-dependent manner (1, 3, 6). These conformational changes generate the power stroke for the walking of kinesin and determine the direction of motion. The comparison of the cryo-EM structures of kinesin in the ATP and ADP states has shown that ATP binding to a microtubule-associated kinesin head causes a conformational change that is believed (7) to tilt the stalk in the forward (plus) direction. Other studies (8, 9) indicate that ADP release might induce redocking of the neck linker and motor stepping.

Biochemical studies have shown that ATP binds to kinesin with a high rate constant of $\approx 4\ \mu M^{-1}\cdot s^{-1}$ (4). The binding of ATP to kinesin is thought (6, 7) to induce a conformational change of the latter. Its switch region (switch I) that flanks the active site shifts between open and closed states (4). Only the closed state is active for ATP hydrolysis. There may be further conformational change of kinesin after ATP hydrolysis, as indicated by the structural difference observed between AMPPNP (adenyl-5′-yl imidodiphosphate, an ATP analogue that hydrolyzes very slowly) and ATP-bound kinesin in fluorescence microscopy (10). The dissociation constant K_d of ATP at its kinesin-binding site is ≈75 μM (4), so ATP dissociates from its binding site with a rate constant of $\approx 150\ s^{-1}$. In the presence of a microtubule, the ATP hydrolysis catalyzed by kinesin is relatively slow, with a rate constant $\approx 6\ s^{-1}$ (4). The release of ADP from a kinesin that is not associated with a microtubule has a rate constant of $\approx 0.002\ s^{-1}$ (11). The rates of ATP hydrolysis (12) and ADP release both increase (13) when kinesin binds a microtubule (to 100–300 and $\approx 20\ s^{-1}$, respectively). It was found that the ADP release from one head is further accelerated to $60–300\ s^{-1}$ when ATP binds to the other head. It is very likely that ADP release is still the rate-limiting step (4, 11) under these conditions. P_i release occurs at a rate of $>100\ s^{-1}$ and is thought not to be rate limiting under any of the conditions mentioned above (4, 14). These studies also showed that a kinesin head with an ADP in its nucleotide site binds to the microtubule weakly [$K_d \approx 10–20\ \mu M$ (4)] and that ADP release from the motor head allows it to bind much more strongly to the microtubule (4, 15).

Single-molecule detachment experiments confirmed that an ADP-occupied kinesin head binds a microtubule much more weakly than a nucleotide-free or AMPPNP-occupied kinesin head (16–18). The experimentally determined unbinding force (the force applied to detach kinesin from a microtubule) for the ADP state is <4 pN (16, 18), whereas the unbinding forces for the empty and AMPPNP states are both >6 pN (18). It was also observed (18) that for all three states, a larger force is needed to detach the kinesin head when it is pulled in the minus direction (the direction opposite to the motion of kinesin) than when it is pulled in the plus direction. The unbinding force of the ADP state is 3.3–3.4 pN with a plus-end load and becomes 3.6–3.9 pN under a minus-end load. The unbinding force of the AMPPNP and empty states is 6.1–6.9 pN in the plus direction and is 9.1–10 pN in the minus direction. These studies also showed that the unbinding force is similar for a monomeric and dimeric kinesin if the heads are at the ADP or empty states, indicating that under these conditions, only one of the two heads of a dimer binds to the microtubule. The observation that when both kinesin heads are occupied by ADP only one head binds the microtubule is consistent with earlier x-ray structural studies (19). In contrast, in the presence of AMPPNP, the detaching force is much larger for a dimer than for a monomer, suggesting that under these conditions, both heads are attached to a microtubule. It is likely

Conflict of interest statement: No conflicts declared.

Abbreviation: AMPPNP, adenyl-5′-yl imidodiphosphate.

*To whom correspondence should be addressed. E-mail: yiqin@mail.chem.tamu.edu.

www.pnas.org/cgi/doi/10.1073/pnas.0602828103

that one of the two heads is occupied by AMPPNP and that the other is empty (18).

It has been observed (20–25) that conventional kinesin is a processive motor and that its step size is ≈8 nm, the axial distance between two adjacent kinesin-binding sites on a microtubule. This step size was shown to be invariant in a large range of ATP concentrations and external loads (20, 22). The stepping of kinesin is tightly coupled to ATP turnover in the presence of both low and high external loads (20). One step of kinesin requires only one ATP molecule, except at very high loads.

A number of different models have been proposed to account for the processive stepping of kinesin (1, 4). In most existing models, ATP binding to an empty kinesin head causes the other head with a bound ADP to move forward, which subsequently reattaches to the microtubule and releases ADP, although the details of these models differ. There have been suggestions of an inchworm model (in which one of the two heads always keeps the leading position), but recent single-molecule experiments convincingly showed that kinesin walks by a hand-over-hand mechanism in which the two heads alternately take the leading position. Using Cy3-labeled kinesin, Yildiz *et al.* (25) showed that each kinesin head takes alternative ≈17-nm and ≈0-nm steps during its walking, with an average step size of the dimer of 8.3 nm. Combined with an earlier observation that kinesin steps are taken without a stalk rotation (26), these results suggest that kinesin walks by an asymmetric hand-over-hand mechanism. The asymmetry of kinesin walking is also consistent with experiments on truncated (27) or mutant homodimeric kinesins (28), which "limp" along the microtubule. The difference in the motions of the two structurally identical monomers suggests that the stepping of kinesin is intrinsically asymmetric, although this asymmetry is not directly observable for a wild-type kinesin (27).

Different research groups have studied the external load as well as ATP concentration dependence of the kinesin motion. Both force-dependent (24) and force-independent (29) Michaelis–Menten constants (the ATP concentration at which the speed of kinesin is one-half of its maximum value obtained at saturating ATP concentrations) have been observed. It has also been observed that kinesin takes not only forward (toward the plus end of the microtubule) but also backward steps (29, 30), with the latter occurring more often with the increase of external load (29, 30). In a recent experiment in which a large range of external loads were applied in both assisting and hindering directions, Carter and Cross (30) observed sustained backward steps of an 8-nm step size at large hindering external forces. The backward steps, similar to the forward steps, are ATP-dependent. Both forward and backward stepping occurs very quickly, on the microsecond time scale, without detectable substeps, in contrast to some earlier experiments (21, 31). To account for the observation of both forward and backward steps, Carter and Cross (30) proposed a model in the prestroke state in which only one head (presumably at an empty state) binds to the microtubule and the other head with an ADP is detached. The latter head takes a position between two microtubule-binding sites along the microtubule axial. ATP binding moves the detached head forward, which subsequently binds to the microtubule and releases ADP; at the same time, the former attached head hydrolyzes ATP and detaches from the microtubule. However, the model is more consistent with a stepping pattern with both steps of a kinesin head being intermediate (between 0 and 17 nm and close to 8 nm), and it is in contradiction to the observation (25) that each of the two heads alternately takes steps of ≈17 nm and ≈0 nm.

Theoretical modeling has proven to be useful in understanding the chemomechanical coupling mechanisms of motor proteins, including kinesin. Both kinetic modeling (32, 33) and master equation approaches (34–36) using thermal ratchet-type models have been used to study the kinetic and mechanical properties of kinesin. However, there has been no detailed physical model to describe the external force and ATP concentration dependence in the hand-over-hand mechanism of kinesin walking on a microtubule (in particular, the backward stepping of kinesin). In the present study, we make use of structural and biochemical experimental data to build a physical model to investigate the hand-over-hand bidirectional movement of kinesin: in particular, the force dependence of the forward/backward ratios, of dwell times, and of the coupling between ATP hydrolysis and kinesin walking. This study provides a physical model that describes these important aspects of kinesin.

A Model of Kinesin

The proposed model of kinesin consists of two heads that are connected through their neck linkers (see Scheme 1). The main assumptions of the present model include the following: (*i*) Each kinesin head binds to the microtubule with an affinity that depends on its chemical state [empty, ADP, or ATP(ADP/P_i) states], with the ATP(ADP/P_i) state possessing the highest binding affinity, and the ADP state being the weakest binding state. The binding affinity of one head is independent of the other. (*ii*) Two reaction coordinates (x_1 and x_2) are used, each for the position of one kinesin head. As shown in Scheme 1, the two heads are connected through their neck linkers. The conformation of the neck linker at each of the chemical states is represented by the angle between the neck linker and the microtubule axis. (*iii*) Three chemical states are considered explicitly [ATP(ADP/P_i), ADP, and empty]. Kinesin, at different chemical states, has stable structures of different angles formed between the neck linker and the microtubule axial. According to cryo-EM studies of single-headed kinesin, the ATP state prefers an angle of ≈45°. The empty head (the rear head) is assumed to take an angle of ≈135° (the exact value depends on the geometry of the kinesin dimer). Because the driving force in the present model results mainly from the ATP-bound kinesin head, this assumption on the structure of the empty state has no significant influence on the results obtained in this study. The ADP state was shown to bind the microtubule weakly and have a flexible neck linker; thus, it does not have preferred angles in the present model. (*iv*) A force exists between the two heads through the interaction between the neck linkers, the conformation of which is determined by the chemical state of the associated motor heads. The motor heads are also subject to the random force due to the thermal noise and the binding force due to their interactions with the microtubule. The details of the model, including the potential energy functions and rate parameters, are given in the supporting information, which is published on the PNAS web site.

Results

Hand-over-Hand Walking of Kinesin. First, we studied the translocation of kinesin along the microtubule in the absence of external forces. A trajectory obtained under such a condition is shown in Fig. 1*a*. Traces for both kinesin heads are shown. One can see from Fig. 1*a* that in the absence of external load, kinesin takes consecutive forward steps (to the plus end of the microtubule), and no backward steps are observed. It can be seen that during the walking of kinesin, the two heads take turns being the leading head. Therefore, kinesin walks by a hand-over-hand mechanism. The maximum speed of kinesin obtained at saturating concentrations of ATP is ≈400 nm·s^{-1}, and the Michaelis–Menten constant, at which ATP concentration the speed of kinesin is one-half of its maximum value, is ≈25 μM. Both parameters are in reasonable agreement with the experimental data of Nishiyama *et al.* (29) but are approximately two and four times, respectively, too small compared with the results of Block and coworkers (24). This difference is likely caused by the different diffusion constants of kinesin in the experimental setup or the different ATP-binding and release constants. The exact origin of

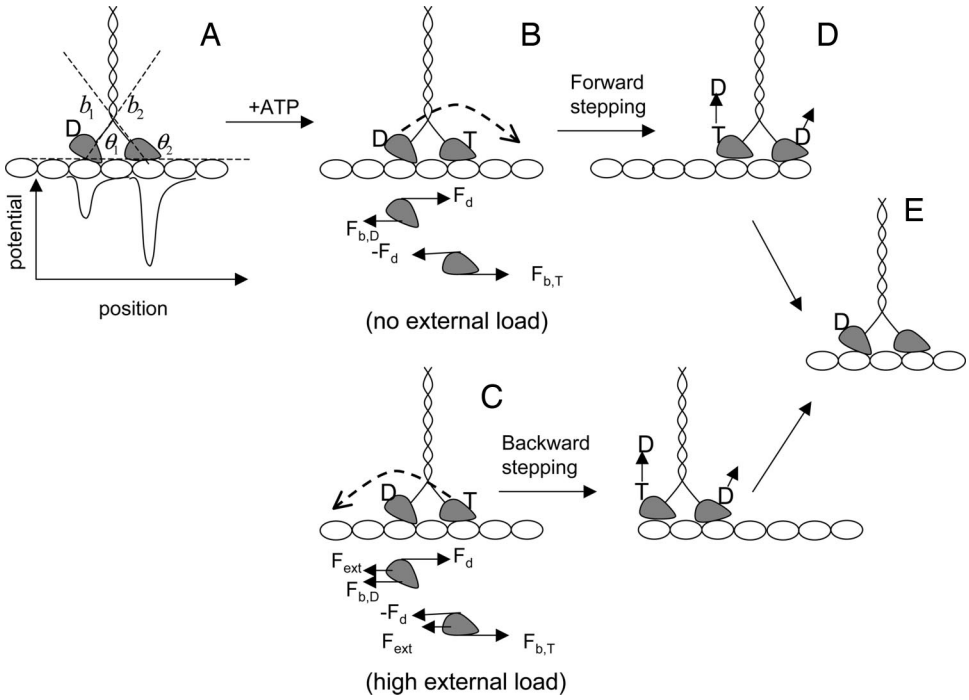

Scheme 1. A schematic model for kinesin and its forward/backward stepping mechanism. State A shows kinesin at the prestroke state. ATP binding (state A to state B and state A to state C) generates a power stroke that exerts a force (F_d) to the plus end for the rear head and a force ($-F_d$) to the minus end for the front head. When the external force is small (state B), because the front head binds the microtubule more strongly, the front head keeps its position, and the rear head moves forward (state B to state D). Because the external force is in the direction opposite to the power stroke on the rear head, these two forces (also the binding force at the microtubule site, $F_{b,D}$) tend to cancel each other, and at large external forces (state C), the rear head holds its position. The external force and the power stroke are both in the minus direction for the front head, and, together, they pull this head off its binding site (against the binding force $F_{b,T}$) and move it in the minus direction (state C to state E). State E is the same chemical state as state A but is generated after either a forward or backward stepping, and ATP binding to state E will lead to either a forward or backward stepping, depending on the external force.

difference is still under investigation. The parameters used in this study allow us to obtain a zero-force speed that falls on the experimental curve of ref. 30. When a force is applied in the minus direction and when it increases, kinesin takes more frequent backward steps (Fig. 1*b*; +7 pN). In the presence of a large enough force, one observes (Fig. 1*c*; +10 pN) sustained backward motions of kinesin with an 8-nm step size and with the two heads alternating the leading position. Therefore, in the presence of large forces, the calculations show a hand-over-hand walking of kinesin to the minus end of the microtubule. Although the speed of the backward motion increases with the force, the motion is slow compared with the forward steps in the absence of external load (≈30 nm/s at +15 pN compared with ≈400 nm/s at 0 pN).

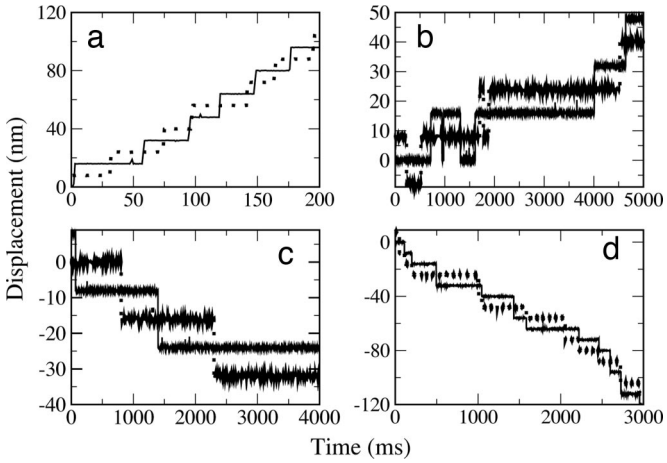

Fig. 1. The trajectory of kinesin motion. Shown are trajectories of kinesin in the absence of external force (*a*) and in the presence of 7 (*b*), 10 (*c*), and 18 (*d*) pN. The trajectories of the two kinesin heads are shown (solid and dotted lines). The ATP concentration is 1 mM.

Force and ATP Concentration Dependence of the Kinesin Speed. To further characterize the external force dependence of kinesin walking, the speed of kinesin is calculated as a function of the external force with 1 mM or 10 μM ATP in solution. As shown in Fig. 2, the applied force influences the kinesin motion in a rather complicated way. Although in general the increase of the

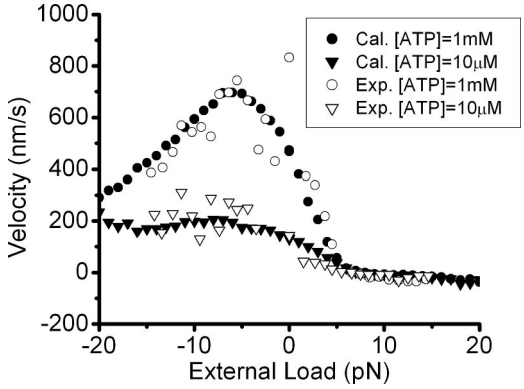

Fig. 2. The velocity of kinesin as a function of the external force. The experimental data are taken from ref. 30.

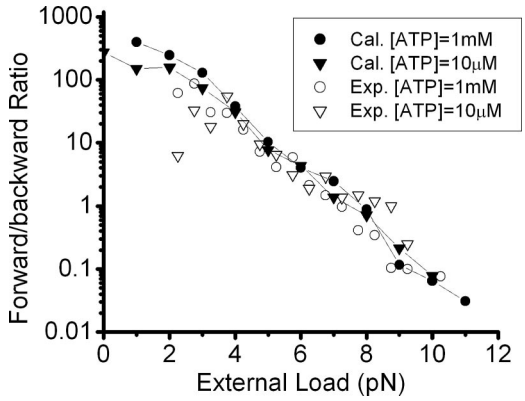

Fig. 3. The forward/backward step ratio as a function of external load. The ATP concentrations are 1 mM and 10 μM, respectively. The experimental data are taken from ref. 30.

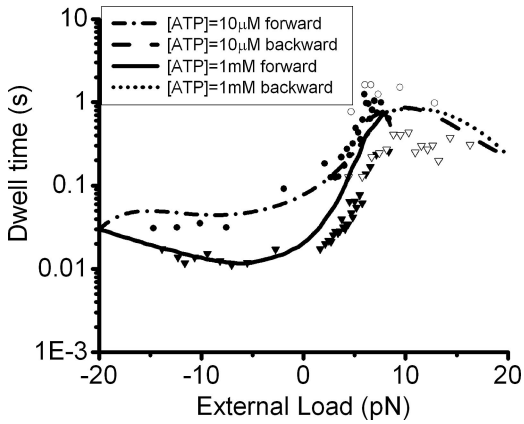

Fig. 4. The dwell times for backward and forward steps as a function of the external force. The ATP concentrations are 1 mM and 10 μM, respectively. The experimental data are taken from ref. 30. The circles represent experimental data obtained with 10 μM ATP (●, forward; ○, backward), and the triangles represent data obtained with 1 mM ATP (▼, forward; ▽, backward).

opposing force decreases the kinesin speed and induces motions in the minus direction, the assisting force does not always increase the kinesin speed. Instead, at an ATP concentration of 1 mM, the speed of kinesin reaches a maximum in the presence of a ≈ -5-pN external load. Further increase (more negative) of the assisting external load decreases the kinesin walking speed (see Fig. 2). This observation is consistent with the experimental results of Carter and Cross (30). In contrast, the speed of kinesin decreases monotonically when the external force changes from 0 to $\approx$7.5 pN (for [ATP] = 1 mM), without changing the direction of net motion.

Forward/Backward Step Ratio and Its Force Dependence. To understand the transition between the forward and backward motions, we studied the external load dependence of the ratio between the numbers of forward and backward steps. The calculations were performed for both 1 mM and 10 μM ATP. As seen from Fig. 3, the difference due to the change of ATP concentration is small, and, in both cases, the forward/backward ratio decreases monotonically with the external force. This ratio becomes unity at the stall force. Therefore, the zero speed of kinesin results from equal numbers of forward and backward steps without cease of motion. The stall force (the force at which the speed of kinesin vanishes) appears to be insensitive to the ATP concentration. The stall force decreases from $\approx$7.5 pN at 1 mM ATP to 7 pN at 10 μM ATP (see the supporting information for more details). These results are in reasonable agreement with the experiments (Fig. 3). Both calculated and experimental results show an almost linear dependence of the forward/backward ratio as a function of the external force.

Dwell Times and Their Dependence on the External Force. Calculations were also performed to study the force dependence of the dwell time between individual steps for both forward and backward motions. This calculation is possible because the physical motion of the kinesin heads occurs on a time scale of 10 μs (30), much faster than the chemical transitions (see Fig. 1). The calculations were again performed for ATP concentrations of 1 mM and 10 μM. The calculated results are shown in Fig. 4. In general, the dwell time is smaller for 1 mM ATP than for 10 μM ATP, indicating that, at least at 10 μM, ATP binding is still rate limiting, consistent with $K_m \approx 30$ μM. In the force range of -15 to 5 pN, the dwell time is insensitive to the external force, although it appears that a minimum of dwell time exists at ≈ -5 pN, consistent with Fig. 2, which shows that maximum speed occurs at ≈ -5 pN. Because of the rareness of backward steps, dwell time of backward steps was calculated only for forces >2 pN. When the external force increases from 5 to 10 pN, we see a sharp increase of the dwell time from $\approx$0.05 s to $\approx$1 s for [ATP] = 1 mM and from $\approx$0.1 to $\approx$1 s for [ATP] = 10 μM. There is no apparent difference in the force dependence of the forward and backward motions, indicating that the forward and backward steps share the same rate-limiting steps. The calculated force dependence of the dwell times agrees reasonably well with experiments. However, unlike the experimental results, the calculated dwell times at large hindering forces (>10 pN) are independent of ATP concentrations in the range of 10 μM to 1 mM. The discrepancy between the calculated and experimental results is likely due to an additional force term that is missing in the present model. This ATP concentration dependence of dwell time indicates that K_m is much higher than 10 μM in this force range, even when the turnover rate of ATP becomes very small because of the slow translocation speed of kinesin. A K_m increasing with the hindering force has been observed in ref. 24 and would require an additional force dependence of the ATP dissociation constant (that increases with external force) (unpublished data).

ATP Hydrolysis Versus Kinesin Stepping. To determine the coupling ratio between ATP hydrolysis and kinesin stepping, the average number of ATPs hydrolyzed for every kinesin step (backward or forward) is calculated as a function of external force. It is seen from Fig. 5 that the chemomechanical coupling ratio is close to unity in a large range of external forces. The higher the ATP concentration, the larger the force range that the tight coupling sustains (-15 to 6 pN for [ATP] = 1 mM and -10 to 6 pN for [ATP] = 10 μM). At large negative forces and a low concentration of ATP, kinesin takes more than one 8-nm step per ATP hydrolyzed, corresponding to a forced sliding in the plus direction. The forced sliding is not seen for [ATP] = 1 mM for forces less negative than -15 pN, suggesting a stronger binding of kinesin to the microtubule in the presence of higher concentrations of ATP. The force dependence of chemomechanical coupling ratios at large positive forces shows a more complicated behavior in the region of the forward/backward stepping transition: Near the stall force, the kinesin stepping becomes loosely coupled to ATP hydrolysis, with more than one ATP consumed for a successful step. Taking into account that the net motion is close to zero in this range of force, this loose coupling is due to the balance between the force produced by kinesin and the external load, which leads to a quick forward/backward motion of one head without moving the other. However, when the force

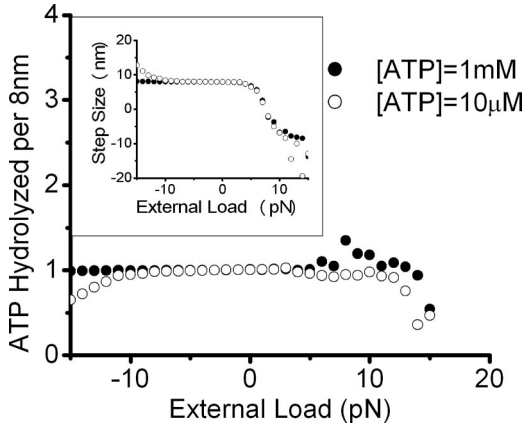

Fig. 5. The chemomechanical coupling ratio and average step size as a function of external force.

further increases, the chemomechanical coupling ratio approaches unity again, indicating the recovery of a tight coupling during the consecutive backward motion in this range of external load. This ratio becomes <1 at even larger hindering forces (>15 pN for [ATP] = 1 mM), and slippage to the minus end of the microtubule occurs (Fig. 1*d*).

Discussion

In this report, we present a simple model for the translocation of kinesin on the microtubule. The main goal of the present work is to understand the recent single-molecule experiments on the mechanical response of kinesin to external loads and to construct a simple theoretical model that will allow us to understand forward and backward motions of kinesin and to make experimentally testable predictions. We have studied the force dependence of both forward and backward stepping of kinesin. The model predicts a hand-over-hand mechanism for kinesin in both small and large forces (−15 to +15 pN for 1 mM ATP), and for motions in both minus and plus directions, given that the ATPase activity of the kinesin head depends only on its conformation. However, when a very large force is applied, one could observe an inchworm walking/sliding mechanism (Fig. 1*d*). It was found that the force up to which the hand-over-hand mechanism sustains decreases when the ATP concentration decreases.

The mechanism of forward kinesin walking in the present theoretical model is, in essence, the same as earlier suggestions (1, 3, 4). In this mechanism, the prestroke state consists of one ADP-occupied and one empty kinesin head. In this prestroke state, the empty head takes the leading position (to the plus direction). Both kinesin heads are bound to the microtubule, and the front one binds more strongly. This feature of the current model is different from that proposed by Carter and Cross (30) and, as shown in Scheme 1, is consistent with the observed 17- and 0-nm alternate steps for each head (25). ATP binding to the front empty head induces a conformational change of its neck linker, which prefers a tilting angle of ≈45° (7, 8) and thus prefers to be the rear head through the interaction between the neck linkers connected to the heads (see Scheme 1). In the absence of a large hindering force, the backward movement of this head is very unlikely because of its strong binding to the microtubule. In contrast, the rear ADP head binds the microtubule weakly and is easily detached. It is thus pulled forward by the front head (bound with ATP) until it reattaches to the next microtubule-binding site, which is ≈17 nm away from its original binding site. This motion makes the original front head (with an ATP bound) a rear one, the neck linker of which therefore redocks to its stable conformation (see Scheme 1, states B–D). The reattachment of the ADP-occupied head further decreases its ADP-binding affinity and allows ADP to be released, whereas ATP hydrolysis and P_i release (both believed to be fast) transform the rear head to the ADP state, which is only weakly bound to the microtubule. Therefore, in the forward motions, through each of the reacting cycles, one of the two heads moves to the plus end of microtubule by ≈17 nm, and the other head stays tightly bound to its microtubule-binding site. ATP binding to the new empty head initiates another cycle of ATP hydrolysis and therefore the next forward step of kinesin, with the two heads exchanging their roles from the previous step. As a result, one observes the hand-over-hand walking mechanism of kinesin.

The model was further used to investigate the influence of the external force on the walking mechanism of kinesin. Consistent with experiments, the hindering forces not only slow down the forward motion of kinesin but also lead to more frequent backward steps, thus decreasing the forward/backward ratio. The backward stepping occurs by the following mechanism: ATP binding to the front head generates a force between the two heads through the neck linkers so that the front head is pulled in the backward direction and the rear head is pulled to the plus direction. When the external force is small, it is the weakly bound rear head that detaches, as discussed earlier. A large hindering force, however, balances with the forward force on the rear head that is generated from the front head and prevents the forward motion of the rear head (Scheme 1, state C). Therefore, a large enough hindering force holds the rear head at its microtubule-binding site. The front head with an ATP bound, however, is subject to the power stroke and the external force, both in the minus-end direction (Scheme 1, state C). These two forces together detach the front head in the ATP state from the microtubule and drive its motion in the minus direction. When this detached head reattaches a microtubule-binding site that is ≈17 nm away from its original binding site, in the minus direction, the driving force due to the power stroke vanishes, and it binds strongly to the microtubule until another ATP binds. As a result, consecutive backward steps are achieved.

What is somewhat surprising in the force dependence of the motion of kinesin is that the assisting force does not always increase the speed of kinesin. In fact, as mentioned earlier, in the force range of ≈−5 to −15 pN, the larger the assisting force, the slower the motor walks. The other surprising result, again consistent with experiments, is that the dwell time of the forward steps and the dwell time of the backward steps both increase with the applied force and that the forward and backward stepping have the same dwell times. These two findings are both consistent with experiments and are easily understood given the stepping mechanism discussed above.

Although the assisting force increases the speed of the physical translocation of kinesin, it also displaces the kinesin heads slightly from their optimal binding positions on the microtubule and slows down the chemical transitions. The observed decrease of kinesin speed with the increase of relatively large assisting force suggests that the rate-limiting steps are chemical rather than physical. Consistently, experiments have shown that the time that is required for a kinesin to take a physical step is in the range of 10 μs for both forward and backward steps (30), much shorter than the overall turnover time (on the order of 10 ms or slower). This observation of the chemical transitions being the rate-limiting steps is also consistent with the force dependence of the dwell times. As shown in Fig. 5, the hindering force has a large effect on the dwell time: The dwell time increases by a factor of ≈20 when the external force increases from 5 to 10 pN ([ATP] = 1 mM). This effect is the same for the forward and backward steps. The increase of the dwell time of the forward step in the presence of an opposing force is in accord with the lower frequency of its occurrence. However, increase of the dwell time of the backward steps accompanies the increase of its

frequency of occurrence. Because in both forward and backward stepping described above ATP hydrolysis occurs in the rear head and ADP releases from the front head (to the plus end), the dwell times of both forward and backward motions show the same force dependence. Therefore, the applied force in the minus direction decreases the overall turnover rate of ATP hydrolysis, and the chemical transitions remain as the rate-limiting steps. Because the chemical states at which the forward and backward stepping take place are the same, the dwell times of forward and backward steps are the same and respond to the external load in the same way.

The force dependence of kinesin discussed above makes it a tightly coupled motor in a large range of external loads. This tight coupling is achieved because in both forward and backward walking, ATP binding to an empty site is required for the detachment of one of the two heads. And in a large range of forces, one of the two heads (in the presence of small forces and forward stepping, it is the front head, and in backward stepping, it is the rear head) binds strongly to the microtubule. Therefore, both forward and backward steps are tightly coupled to ATP turnover. It is because of this tight coupling that the stall force does not depend on the ATP concentration sensitively. These properties of kinesin make it a strong motor with high efficiency when it walks against large forces and ensure that kinesin can sustain a large negative force. Even when the force is much larger than the stall force (>10 pN), kinesin steps backward with a slow speed in an ATP-dependent manner, instead of sliding backward quickly or detaching from the microtubule (see Fig. 2). The tight chemomechanical coupling mechanism of kinesin is very different from that of the other microtubule-based motor protein, cytoplasm dynein. The latter walks to the minus end of the microtubule and possesses a loose chemomechanical coupling mechanism in that it responds to an external load as a gear, and its stall force depends strongly on the ATP concentration (37, 38). The difference between the two motors may be a result of their different origins. It is also likely that each possesses its mechanical/chemical properties to fulfill its unique biological function. Detailed structural and biochemical studies may shed more light on the molecular mechanisms of these motor proteins and may provide the necessary test of the mechanistic model that we present here.

Finally, we note that to take into account the asymmetric hand-over-hand walking that has been observed for mutant kinesins, the neck linkers of the heads are assumed in the present study to have different lengths, and each of them also depends on which of the two heads is in the front position (see the supporting information). The present model with parameters given in the supporting information does not show asymmetry in the walking of kinesin. However, further shortening of the neck linkers by mutation amplifies the difference between the neck linkers of the two heads and brings out more apparently the asymmetry in kinesin walking (unpublished data).

We thank Drs. Carter and Cross (both at Molecular Motors Group, Marie Curie Research Institute, Surrey, England) for providing experimental data. This work was supported by a Texas A&M University startup grant and a Camille and Henry Dreyfus Foundation New Faculty Award (both to Y.Q.G.). For computations, we used the Tensor Cluster at Texas A&M University, which was purchased under National Science Foundation Grant DMS 0216275.

1. Yildiz, A. & Selvin, P. L. (2005) *Trends Cell Biol.* **15,** 112–120.
2. Hirokawa, N. (1998) *Science* **279,** 519–526.
3. Asbury, C. L. (2005) *Curr. Opin. Cell Biol.* **17,** 89–97.
4. Cross, R. A. (2004) *Trends Biochem. Sci.* **29,** 301–309.
5. Vale, R. D. (2003) *Cell* **112,** 467–480.
6. Cross, R. A., Crevel, I., Carter, N. J., Alonso, M. C., Hirose, K. & Amos, L. A. (2000) *Philos. Trans. R. Soc. London Ser. B* **355,** 459–464.
7. Rice, S., Lin, A. W., Safer, D., Hart, C. L., Naber, N., Carragher, B. O., Cain, S. M., Pechatnikova, E., Wilson-Kubalek, E. M., Whittaker, M., *et al.* (1999) *Nature* **402,** 778–784.
8. Hirose, K., Lockhart, A., Cross, R. A. & Amos, L. A. (1995) *Nature* **376,** 277–279.
9. Yun, M., Bronner, C. E. & Park, C. G. (2003) *EMBO J.* **22,** 5382–5389.
10. Asenjo, A. B., Krohn, N. & Sosa, H. (2003) *Nat. Struct. Biol.* **10,** 836–842.
11. Kull, F. J. & Endow, S. A. (2002) *J. Cell Sci.* **115,** 15–23.
12. Hackney, D. D. (1988) *Proc. Natl. Acad. Sci. USA* **85,** 6314–6318.
13. Ma, Y. Z. & Taylor, E. W. (1997) *J. Biol. Chem.* **272,** 717–723.
14. Lockhart, A., Cross, R. A. & McKillop, D. F. (1995) *FEBS Lett.* **368,** 531–535.
15. Xing, J., Wriggers, W., Jefferson, G. M., Stein, R., Cheung, H. C. & Rosenfeld, S. S. (2000) *J. Biol. Chem.* **275,** 25413–25423.
16. Kawaguchi, I. & Ishiwata, S. (2001) *Science* **291,** 667–669.
17. Kawaguchi, K., Uemura, S. & Ishiwata, S. (2003) *Biophys. J.* **84,** 1103–1113.
18. Uemura, S., Kawaguchi, K., Yajima, J., Edamatsu, M., Toyoshima, Y. Y. & Ishiwata, S. (2002) *Proc. Natl. Acad. Sci. USA* **99,** 5977–5981.
19. Kozielski, F., Sack, S., Marx, A., Thormahlen, M., Schonbrunn, E., Biou, V., Thompson, A., Mandelkow, E. M. & Mandelkow, E. (1997) *Cell* **91,** 985–994.
20. Coy, D. L., Wagenbach, M. & Howard, J. (1999) *J. Biol. Chem.* **274,** 3667–3671.
21. Nishiyama, M., Muto, E., Inoue, Y., Yanagida, T. & Higuchi, H. (2001) *Nat. Cell Biol.* **3,** 425–428.
22. Schnitzer, M. J. & Block, S. M. (1997) *Nature* **388,** 386–390.
23. Schnitzer, M. J., Visscher, K. & Block, S. M. (2000) *Nat. Cell Biol.* **2,** 718–723.
24. Visscher, K., Schnitzer, M. J. & Block, S. M. (1999) *Nature* **400,** 184–189.
25. Yildiz, A., Tomishige, M., Vale, R. D. & Selvin, P. R. (2004) *Science* **303,** 676–678.
26. Hua, W., Chung, J. & Gelles, J. (2002) *Science* **295,** 844–848.
27. Asbury, C. L., Fehr, A. N. & Block, S. M. (2003) *Science* **302,** 2130–2134.
28. Higuchi, H., Bronner, C. E., Park, H. W. & Endow, S. A. (2004) *EMBO J.* **23,** 2993–2999.
29. Nishiyama, M., Higuchi, H. & Yanagida, T. (2002) *Nat. Cell Biol.* **4,** 790–797.
30. Carter, N. J. & Cross, R. A. (2005) *Nature* **435,** 308–312.
31. Coppin, C. M., Finer, J. T., Spudich, J. A. & Vale, R. D. (1996) *Proc. Natl. Acad. Sci. USA* **93,** 1913–1917.
32. Fisher, M. E. & Kolomeisky, A. B. (2001) *Proc. Natl. Acad. Sci. USA* **98,** 7748–7753.
33. Kolomeisky, A. B., Stukalin, E. B. & Popov, A. A. (2005) *Phys. Rev. E* **71,** 031902.
34. Astumian, R. D. (2000) *Philos. Trans. R. Soc. London Ser. B* **355,** 511–522.
35. Peskin, C. S. & Oster, G. (1995) *Biophys. J.* **68,** S202–S211.
36. Thomas, N., Imafuku, Y., Kamiya, T. & Tawada, K. (2002) *Proc. R. Soc. London Ser. B* **269,** 2363–2371.
37. Gao, Y. Q. (2006) *Biophys. J.*, **90,** 811–821.
38. Mallik, R., Carter, B. C., Lex, S. A., King, S. J. & Gross, S. P. (2004) *Nature* **427,** 649–652.